Ionization of H_2^+ molecular ions by twisted Bessel light

A. A. Peshkov,[1,*] S. Fritzsche,[1,2] and A. Surzhykov[1]
[1]*Helmholtz-Institut Jena, D-07743 Jena, Germany*
[2]*Theoretisch-Physikalisches Institut, Abbe Center of Photonics, Friedrich-Schiller-Universität Jena, D-07743 Jena, Germany*
(Received 10 August 2015; published 20 October 2015)

The photoionization of H_2^+ molecular ions is investigated for Bessel beams of twisted light. In particular, the angle-differential photoionization cross sections are evaluated for a macroscopic target of randomly distributed but initially aligned ions by using the nonrelativistic first-order perturbation theory. Detailed calculations of these cross sections and angular distributions are performed for different setups of the electron detectors and for selected opening angles of the Bessel beams and are compared with those for incident plane-wave radiation. It is shown that the modification in the angular distributions of the photoelectrons can be understood quite easily from the variations in the intensity pattern of the Bessel beams, relative to the size of the H_2^+ molecular ions.

DOI: 10.1103/PhysRevA.92.043415 PACS number(s): 33.80.Eh

I. INTRODUCTION

Like in Young's well-known double-slit experiment with plane-wave light, interference effects have been observed and discussed also in the photoionization of diatomic molecules [1,2]. These interferences in the photoelectron spectra can be understood quite easily in terms of the phase shift of the electrons, if they are emitted from different (atomic) centers of the molecule. These interference phenomena were first analyzed by Cohen and Fano [3] almost half a century ago and since then the photoionization of diatomic molecules has been intensively explored in both experiment and theory [4,5]. These investigations gave rise to valuable information about the molecular structure [6,7] as well as the angular distributions of photoelectrons for their interaction with light of different frequency and intensity [8,9].

Until the present, however, all molecular double-slit experiments have been performed with incident plane-wave radiation. Very little is known about the photoionization of (diatomic) molecules by beams of twisted (or vortex) light, which have become available during recent years [10–14]. In contrast to plane-wave radiation, such twisted photons carry a nonzero projection of the orbital angular momentum (OAM) upon their propagation direction. In addition, these twisted beams also exhibit a quite distinguished inhomogeneous intensity profile, if taken in the plane perpendicular to the propagation direction of the beam [15–17]. We can therefore expect [18–24] that the OAM and intensity profile of such beams will affect also the cross sections and angular distributions of the photoelectrons in the photoionization of (diatomic) molecules.

In this paper we investigate theoretically the photoionization of H_2^+ molecular ions for Bessel beams of twisted light. Nonrelativistic first-order perturbation theory is applied, along with Born's approximation, in order to analyze the cross sections and angular distributions of the emitted photoelectrons. In particular, we here compare and discuss the basic formulas for the (angle-differential) photoionization cross sections for incident plane waves (Sec. II A) and twisted light (Sec. II B). For the sake of simplicity, however, we restrict ourselves to just a macroscopic target of H_2^+ molecules that are randomly distributed but all aligned with regard to the propagation direction of the incident beam. Detailed calculations were performed for different orientations (alignments) of the molecular ions and for different photon energies. In Sec. III we present our results and show that the known oscillations in the angular and energy distributions of photoelectrons, as they were confirmed in experiments with plane-wave radiation [8], become much less pronounced for twisted light. This loss of interference in the photoionization cross sections and angular distributions appears especially if the variations in the intensity profile of the beams become comparable to the size of the H_2^+ molecular ions, i.e., at higher photon energies. Both the energy and angular dependence of the predicted photoelectron spectra will be discussed in detail. Finally, a summary and outlook are given in Sec. IV.

Hartree atomic units ($\hbar = 4\pi\varepsilon_0 = e = m_e = 1, c = 1/\alpha$, where α is a fine-structure constant) are used throughout the paper unless stated otherwise.

II. THEORY

Let us start from the general transition amplitude that describes the photoionization of a H_2^+ molecular ion, which consists of just two nuclei (protons) and a single electron. In first-order perturbation theory, the differential and total (photoionization) cross sections are usually expressed in terms of the (transition) matrix element [25]

$$M_{fi} = -i \int \psi_f^*(\boldsymbol{r}) \boldsymbol{A}(\boldsymbol{r}) \cdot \nabla \psi_i(\boldsymbol{r}) d^3\boldsymbol{r} \qquad (1)$$

that describes the transition of the electron from its initial bound state ψ_i into the final continuum state ψ_f because of the absorption of an incident photon. Here all the properties of the photons are characterized by means of the vector potential $\boldsymbol{A}(\boldsymbol{r})$. Therefore, in order to calculate the transition amplitude (1), we need to know the explicit form of the wave functions of the electron in its initial and final states as well as the vector potential of the incident light field. As usual, we here construct the initial wave function ψ_i of the $1\sigma_g$ molecular ground state as a linear combination of atomic orbitals

$$\psi_i(\boldsymbol{r}) = \tfrac{1}{\sqrt{2}}[\psi_{1s}(\boldsymbol{r} - \boldsymbol{R}/2) + \psi_{1s}(\boldsymbol{r} + \boldsymbol{R}/2)], \qquad (2)$$

*anton.peshkov@uni-jena.de

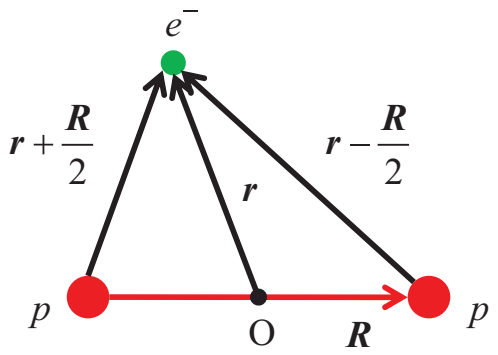

FIG. 1. (Color online) Coordinates that are used to describe the hydrogen molecular ion H_2^+. If the origin is chosen at the midpoint of the internuclear axis, the position vector $\boldsymbol{r}$ of the electron can easily be written also in terms of the positions of the two nuclei as $\boldsymbol{r} \pm \boldsymbol{R}/2$.

where ψ_{1s} denotes the $1s$ ground-state orbital of atomic hydrogen [25]. Moreover, $\boldsymbol{R}$ is the (internuclear) vector from the first proton to the second, and $\boldsymbol{r}$ is the position vector of the electron with regard to the origin of the coordinates (cf. Fig. 1).

In the first-order Born approximation, which is applied in this work, a plane wave

$$\psi_f(\boldsymbol{r}) = (2\pi)^{-3/2} e^{i\boldsymbol{p}_f \cdot \boldsymbol{r}} \tag{3}$$

is supposed for the outgoing electron with momentum $\boldsymbol{p}_f$ in the matrix element (1). This approximation is valid when the kinetic energy T_f of the emitted electron is large compared to its interaction with the remaining nuclei, but (much) smaller than the rest energy of the electron

$$I_p \ll T_f \ll m_e c^2. \tag{4}$$

In addition, the photon energy ω, ionization potential I_p of the H_2^+ molecular ion, and the (modulus of the) momentum are related to each other by

$$T_f = \frac{p_f^2}{2} = \omega - I_p, \tag{5}$$

due to energy conservation.

Indeed, the first-order Born approximation (3) has often been utilized to analyze the photoionization of diatomic molecules. For low-Z targets and high photon energies $\hbar\omega \gtrsim 200$ eV, this approach was found to be adequate for the computation of both the total and angle-differential photoionization cross sections [26–28]. In particular, the interference behavior of the cross sections, obtained for the plane wave (3), has been reproduced by more accurate calculations based, for example, on the B-spline basis functions for the continuum electron spectrum. Since in the present study we aim to elucidate the major effects arising in the ionization of molecules by twisted photon beams, we will use the simple first-order Born approximation for the incident photons with energies $\hbar\omega > 200$ eV.

Apart from the wave functions ψ_i and ψ_f, we need to know the vector potential $\boldsymbol{A}(\boldsymbol{r})$ for evaluating the transition amplitude (1) whose explicit form depends of course on the (properties of the) incident radiation. In the following sections we analyze and compare this matrix element for plane-wave radiation as well as for twisted Bessel light.

A. Ionization by plane-wave photons

The ionization of H_2^+ molecular ions by a plane wave has been discussed in detail; see, for example, Ref. [7]. Here we therefore restrict ourselves to a rather short account of the basic formulas. For plane-wave light with photon energy $\omega = k/\alpha$ and helicity $\lambda = \pm 1$, the vector potential is given by

$$\boldsymbol{A}^{\rm pl}(\boldsymbol{r}) = \boldsymbol{e}_{k\lambda} e^{i\boldsymbol{k}\cdot\boldsymbol{r}}, \tag{6}$$

where $\boldsymbol{e}_{k\lambda}$ denotes the polarization vector. If we insert this potential (6) into Eq. (1), we then obtain the transition amplitude

$$M_{fi}^{\rm pl}(\boldsymbol{k}) = -i \int \psi_f^*(\boldsymbol{r}) e^{i\boldsymbol{k}\cdot\boldsymbol{r}} \boldsymbol{e}_{k\lambda} \cdot \nabla \psi_i(\boldsymbol{r}) d^3\boldsymbol{r}. \tag{7}$$

To further simplify this amplitude, we can rewrite Eq. (7) as

$$\begin{aligned} M_{fi}^{\rm pl}(\boldsymbol{k}) &= -i \int {\rm div}[\psi_f^*(\boldsymbol{r}) e^{i\boldsymbol{k}\cdot\boldsymbol{r}} \boldsymbol{e}_{k\lambda} \psi_i(\boldsymbol{r})] d^3\boldsymbol{r} \\ &\quad + i \int \boldsymbol{e}_{k\lambda} \psi_i(\boldsymbol{r}) \cdot \nabla[\psi_f^*(\boldsymbol{r}) e^{i\boldsymbol{k}\cdot\boldsymbol{r}}] d^3\boldsymbol{r} \\ &= -i \oint \psi_f^*(\boldsymbol{r}) e^{i\boldsymbol{k}\cdot\boldsymbol{r}} \boldsymbol{e}_{k\lambda} \psi_i(\boldsymbol{r}) d^2\boldsymbol{S} \\ &\quad + i \int \boldsymbol{e}_{k\lambda} \psi_i(\boldsymbol{r}) \cdot \nabla[\psi_f^*(\boldsymbol{r}) e^{i\boldsymbol{k}\cdot\boldsymbol{r}}] d^3\boldsymbol{r}, \end{aligned} \tag{8}$$

where, in the third line, we made use of Gauss's integral theorem to rewrite the integral over the volume into a surface integral, though for an infinite volume. Since the initial state decays rapidly to zero $\psi_i(\boldsymbol{r}) \to 0$ for $r \to \infty$, this surface integral just vanishes. Hence, the transition amplitude can be written as

$$M_{fi}^{\rm pl}(\boldsymbol{k}) = -\frac{\boldsymbol{e}_{k\lambda} \cdot \boldsymbol{p}_f}{(2\pi)^{3/2}} \int e^{i(\boldsymbol{k}-\boldsymbol{p}_f)\cdot\boldsymbol{r}} \psi_i(\boldsymbol{r}) d^3\boldsymbol{r}. \tag{9}$$

Here we have employed the final-state wave function (3) and the orthogonality between the polarization and the wave vectors of a photon $\boldsymbol{e}_{k\lambda} \cdot \boldsymbol{k} = 0$.

We can further apply the initial wave function (2) as well as the well-known Fourier transform of the hydrogenic $1s$ ground state [29]

$$\int e^{i(\boldsymbol{k}-\boldsymbol{p}_f)\cdot\boldsymbol{r}} \psi_{1s}(\boldsymbol{r}) d^3\boldsymbol{r} = \frac{8\sqrt{\pi}}{[(\boldsymbol{k}-\boldsymbol{p}_f)^2 + 1]^2} \tag{10}$$

to finally obtain the (known) transition amplitude for the photoionization of H_2^+ molecular ions as

$$M_{fi}^{\rm pl}(\boldsymbol{k}) = -\frac{4}{\pi} \frac{\boldsymbol{e}_{k\lambda} \cdot \boldsymbol{p}_f}{[(\boldsymbol{k}-\boldsymbol{p}_f)^2 + 1]^2} \cos\left[\frac{(\boldsymbol{k}-\boldsymbol{p}_f)\cdot\boldsymbol{R}}{2}\right]. \tag{11}$$

In fact, the matrix element (11) can be utilized to express and obtain all properties of the photoionization process. For example, the angle-differential cross section is simply given by

$$\begin{aligned} \frac{d\sigma^{\rm pl}}{d\Omega_f} &= \frac{2\pi p_f}{j^{\rm pl}} \left| M_{fi}^{\rm pl}(\boldsymbol{k}) \right|^2 \\ &= \frac{32\alpha p_f}{\omega} \frac{|\boldsymbol{e}_{k\lambda} \cdot \boldsymbol{p}_f|^2}{[(\boldsymbol{k}-\boldsymbol{p}_f)^2 + 1]^4} \{1 + \cos[(\boldsymbol{k}-\boldsymbol{p}_f)\cdot\boldsymbol{R}]\}, \end{aligned} \tag{12}$$

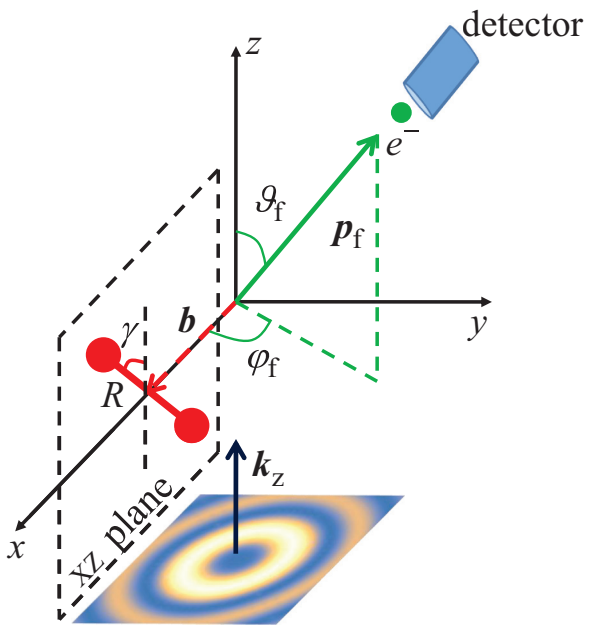

FIG. 2. (Color online) Geometry for the ionization of H_2^+ molecules by twisted light. While the quantization axis (z axis) is taken along the propagation direction of the incident beam, the H_2^+ molecular ion is supposed to lie in the xz plane. Moreover, the molecule is aligned with angle γ with respect to the z axis and its center (of mass), i.e., the origin of the intermolecular coordinates, is displaced by the impact parameter $\boldsymbol{b}$ from the beam axis. Finally, the two angles ϑ_f and φ_f describe the detector for observing the emitted photoelectrons.

where $j^{\rm pl} = \omega/(2\pi\alpha)$ is the flux of the incident plane-wave radiation [25].

To further evaluate the angle-differential cross section $d\sigma^{\rm pl}/d\Omega_f$, we first need to agree about the geometry under which the photoelectrons are observed. If we choose the z axis along the direction of the incident light, we can write the wave and polarization vectors of the photons as

$$\boldsymbol{e}_{k\lambda} = \frac{-\lambda}{\sqrt{2}}\begin{pmatrix}1\\ i\lambda\\ 0\end{pmatrix}, \quad \boldsymbol{k} = \begin{pmatrix}0\\ 0\\ k\end{pmatrix}. \tag{13}$$

Moreover, if we assume the internuclear vector $\boldsymbol{R}$ to lie within the xz plane and to be tilted by the angle γ with regard to the z axis (cf. Fig. 2), the differential cross section (12) can be expressed in terms of the angles (ϑ_f,φ_f) of the emitted electron as

$$\frac{d\sigma^{\rm pl}}{d\Omega_f} \approx \frac{16\alpha p_f^3}{\omega}\frac{\sin^2\vartheta_f}{\left[p_f^2+1\right]^4}[1+\cos\eta(k)] \tag{14}$$

with

$$\eta(k) = Rk\cos\gamma - Rp_f[\sin\gamma\sin\vartheta_f\cos\varphi_f + \cos\gamma\cos\vartheta_f]. \tag{15}$$

Here we made use of the relations (4) and (5) to obtain the condition $p_f/(2c) = k/p_f \ll 1$ for not too slow electrons and to write $(\boldsymbol{k}-\boldsymbol{p}_f)^2+1 \approx p_f^2+1$ in the denominator of Eq. (12).

B. Ionization by twisted Bessel light

1. Transition matrix element

We next analyze the ionization of H_2^+ molecular ions by twisted Bessel light with well-defined longitudinal momentum k_z, the (modulus of the) transverse momentum $\varkappa$, and the projection m of the total angular momentum (TAM) upon the quantization axis z. For such a Bessel state of light, the vector potential is given by [15]

$$\boldsymbol{A}^{\rm tw}_{\varkappa m k_z\lambda}(\boldsymbol{r}) = \int a_{\varkappa m}(\boldsymbol{k}_\perp)\boldsymbol{e}_{k\lambda}e^{i\boldsymbol{k}\cdot\boldsymbol{r}}\frac{d^2\boldsymbol{k}_\perp}{(2\pi)^2} \tag{16}$$

and together with the amplitude

$$a_{\varkappa m}(\boldsymbol{k}_\perp) = \sqrt{\frac{2\pi}{\varkappa}}(-i)^m e^{im\phi_k}\delta(k_\perp-\varkappa). \tag{17}$$

As can be seen from these expressions, such a Bessel beam can be understood also as a superposition of plane waves whose wave vectors

$$\boldsymbol{k} = \begin{pmatrix}k_\perp\cos\phi_k\\ k_\perp\sin\phi_k\\ k_z\end{pmatrix} \tag{18}$$

form the surface of a cone and with the polarization vectors

$$\boldsymbol{e}_{k\lambda} = \frac{-\lambda}{\sqrt{2}}\begin{pmatrix}\cos\theta_k\cos\phi_k - i\lambda\sin\phi_k\\ \cos\theta_k\sin\phi_k + i\lambda\cos\phi_k\\ -\sin\theta_k\end{pmatrix}, \tag{19}$$

respectively. In Eq. (19), moreover, we have introduced the so-called opening angle θ_k with $\tan\theta_k = \varkappa/k_z$ to characterize the ratio of the transverse to the longitudinal momenta of the photons in the Bessel beam [18].

The integration over $\boldsymbol{k}_\perp$ in Eq. (16) can be carried out explicitly for Bessel beams and gives rise to a vector potential in the form

$$\boldsymbol{A}^{\rm tw}_{\varkappa m k_z\lambda}(\boldsymbol{r}) = \sum_{m_s=0,\pm1}\boldsymbol{C}_{m_s}(\theta_k)J_{m-m_s}(\varkappa r_\perp)e^{i(m-m_s)\phi}e^{ik_z z}, \tag{20}$$

where the vectors $\boldsymbol{C}_{m_s}(\theta_k)$ were defined in Eq. (25) of Ref. [15], and the $J_n(\varkappa r_\perp)$ denote Bessel functions of the first kind. Equation (20) implies that, in contrast to an incident plane wave, the Bessel light always has an inhomogeneous intensity distribution perpendicular to its propagation direction, i.e., in the xy plane for the given geometry. In Ref. [15] it was furthermore shown that this profile has a concentric ring structure and that, consequently, the photoionization will depend on the position of the H_2^+ molecular ion with regard to the beam axis. We use here the impact parameter $\boldsymbol{b}$ in order to designate the origin of the molecular coordinates with regard to the beam axis (cf. Fig. 2). With this notation, the initial wave function of the electron can be written also as

$$\psi_i(\boldsymbol{r};\boldsymbol{b}) = \tfrac{1}{\sqrt{2}}[\psi_{1s}(\boldsymbol{r}-\boldsymbol{R}/2-\boldsymbol{b}) + \psi_{1s}(\boldsymbol{r}+\boldsymbol{R}/2-\boldsymbol{b})]. \tag{21}$$

Using this wave function and the vector potential (16), we can express the transition amplitude for the ionization of the H_2^+

molecular ions by twisted Bessel light as

$$M_{fi}^{\rm tw}(\boldsymbol{k};\boldsymbol{b}) = -i \int a_{\varkappa m}(\boldsymbol{k}_\perp)\frac{d^2\boldsymbol{k}_\perp}{(2\pi)^2}\int \psi_f^*(\boldsymbol{r})e^{i\boldsymbol{k}\cdot\boldsymbol{r}}\boldsymbol{e}_{\boldsymbol{k}\lambda} \cdot\boldsymbol{\nabla}\psi_i(\boldsymbol{r};\boldsymbol{b})d^3\boldsymbol{r}. \quad (22)$$

This amplitude can be evaluated quite similarly to the plane-wave case [cf. Eqs. (7)–(11)]

$$\begin{aligned} M_{fi}^{\rm tw}(\boldsymbol{k};\boldsymbol{b}) &= -\frac{4}{\pi}\int a_{\varkappa m}(\boldsymbol{k}_\perp)e^{i(\boldsymbol{k}-\boldsymbol{p}_f)\cdot\boldsymbol{b}}\frac{\boldsymbol{e}_{\boldsymbol{k}\lambda}\cdot\boldsymbol{p}_f}{[(\boldsymbol{k}-\boldsymbol{p}_f)^2+1]^2} \\ &\quad\times\cos\left[\frac{(\boldsymbol{k}-\boldsymbol{p}_f)\cdot\boldsymbol{R}}{2}\right]\frac{d^2\boldsymbol{k}_\perp}{(2\pi)^2} \\ &= \int a_{\varkappa m}(\boldsymbol{k}_\perp)e^{i(\boldsymbol{k}-\boldsymbol{p}_f)\cdot\boldsymbol{b}}M_{fi}^{\rm pl}(\boldsymbol{k})\frac{d^2\boldsymbol{k}_\perp}{(2\pi)^2} \end{aligned} \quad (23)$$

and hence finally in terms of the plane-wave transition amplitude $M_{fi}^{\rm pl}(\boldsymbol{k})$ from Eq. (11).

2. *Differential photoionization cross section*

We can apply the amplitude (23) to evaluate the differential photoionization cross section. In contrast to an incident plane wave with a constant flux (per unit area), however, the cross section now depends on the particular geometry under which the incident beam interacts with the target molecules. For instance, if we assume a macroscopic target of initially aligned molecules that are uniformly distributed in their impact parameter $\boldsymbol{b}$ over the extent of the Bessel beam with radius $R_{\rm tw}$, the angle-differential cross section can be determined explicitly by calculating the integral for just $b < R_{\rm tw}$,

$$\begin{aligned} \frac{d\sigma^{\rm tw}}{d\Omega_f} &= \frac{2\pi p_f}{j^{\rm tw}}\int \left|M_{fi}^{\rm tw}(\boldsymbol{k};\boldsymbol{b})\right|^2\frac{d^2\boldsymbol{b}}{\pi R_{\rm tw}^2} \\ &= \frac{4\pi^4\alpha p_f R_{\rm tw}}{\omega\cos\theta_k}\int e^{i(\boldsymbol{k}_\perp-\boldsymbol{k}'_\perp)\cdot\boldsymbol{b}}a_{\varkappa m}(\boldsymbol{k}_\perp)a_{\varkappa m}^*(\boldsymbol{k}'_\perp) \\ &\quad\times M_{fi}^{\rm pl}(\boldsymbol{k})M_{fi}^{\rm pl*}(\boldsymbol{k}')\frac{d^2\boldsymbol{k}_\perp}{(2\pi)^2}\frac{d^2\boldsymbol{k}'_\perp}{(2\pi)^2}\frac{d^2\boldsymbol{b}}{\pi R_{\rm tw}^2}, \end{aligned} \quad (24)$$

where $j^{\rm tw} = \omega\cos\theta_k/(2\pi^3 R_{\rm tw}\alpha)$ denotes the flux of the incident twisted-wave radiation [18].

As can be seen from Eq. (24), the integral over the impact parameter $\boldsymbol{b}$ is proportional to the δ function $\delta(\boldsymbol{k}'_\perp - \boldsymbol{k}_\perp)$ due to the factor $\exp[i(\boldsymbol{k}_\perp - \boldsymbol{k}'_\perp)\cdot\boldsymbol{b}]$ in the integrant. Moreover, by carrying out the trivial integration over $\boldsymbol{k}'_\perp$ and by making use of Eqs. (11) and (17), we find

$$\begin{aligned} \frac{d\sigma^{\rm tw}}{d\Omega_f} &= \frac{32\pi a p_f}{\omega\cos\theta_k R_{\rm tw}}\int\frac{\delta^2(k_\perp-\varkappa)}{\varkappa}\frac{|\boldsymbol{e}_{\boldsymbol{k}\lambda}\cdot\boldsymbol{p}_f|^2}{[(\boldsymbol{k}-\boldsymbol{p}_f)^2+1]^4} \\ &\quad\times\{1+\cos[(\boldsymbol{k}-\boldsymbol{p}_f)\cdot\boldsymbol{R}]\}\frac{d^2\boldsymbol{k}_\perp}{2\pi}. \end{aligned} \quad (25)$$

Furthermore, since we can treat the square of the δ function as [18]

$$\delta^2(k_\perp-\varkappa) = \frac{R_{\rm tw}}{\pi}\delta(k_\perp-\varkappa), \quad (26)$$

the integration over $k_\perp$ in Eq. (25) gives rise to $k_\perp = \varkappa$, and the angle-differential cross section for the photoionization of aligned H_2^+ molecular ions becomes

$$\begin{aligned} \frac{d\sigma^{\rm tw}}{d\Omega_f} &= \frac{32\alpha p_f}{\omega\cos\theta_k}\int_0^{2\pi}\frac{|\boldsymbol{e}_{\boldsymbol{k}\lambda}\cdot\boldsymbol{p}_f|^2}{[(\boldsymbol{k}-\boldsymbol{p}_f)^2+1]^4} \\ &\quad\times\{1+\cos[(\boldsymbol{k}-\boldsymbol{p}_f)\cdot\boldsymbol{R}]\}\frac{d\phi_k}{2\pi}. \end{aligned} \quad (27)$$

If, in addition, we assume the emitted electron to be fast but still nonrelativistic [cf. Eq. (4)], we can rewrite $(\boldsymbol{k}-\boldsymbol{p}_f)^2+1 \approx p_f^2+1$ in the denominator of Eq. (27) and apply the integral representation of the Bessel function [30]

$$J_n(\xi) = \frac{1}{2\pi}\int_\mu^{2\pi+\mu} e^{i(n\phi_k - \xi\sin\phi_k)}d\phi_k \quad (28)$$

in order to perform the integration over the angle ϕ_k in the cross section (27). With these substitutions, the angle-differential cross section for the photoionization of H_2^+ ions by a Bessel beam can be expressed in good approximation as

$$\begin{aligned} \frac{d\sigma^{\rm tw}}{d\Omega_f} &\approx \frac{8\alpha p_f^3}{\omega\cos\theta_k}\frac{1}{\left[p_f^2+1\right]^4}\{[2\sin^2\vartheta_f + 2\sin^2\theta_k \\ &\quad - 3\sin^2\vartheta_f\sin^2\theta_k][1+J_0(R\varkappa\sin\gamma)\cos\eta(k_z)] \\ &\quad + \sin(2\theta_k)\sin(2\vartheta_f)\cos\varphi_f J_1(R\varkappa\sin\gamma)\sin\eta(k_z) \\ &\quad + \sin^2\vartheta_f\sin^2\theta_k\cos(2\vartheta_f)J_2(R\varkappa\sin\gamma)\cos\eta(k_z)\}, \end{aligned} \quad (29)$$

where $\eta(k_z)$ is given by Eq. (15) with $k = k_z$. We here note that, for $\varkappa = 0$ or zero opening angle $\theta_k = 0^\circ$, the expression (27) simply becomes the cross section for the ionization of H_2^+ ions by plane-wave radiation (14) in agreement with the formal limit of a Bessel beam for $\theta_k = 0^\circ$, i.e., for $\boldsymbol{k} \parallel z$.

III. RESULTS AND DISCUSSION

In the previous section we found that the angle-differential cross section for the photoionization of an macroscopic target of aligned but randomly distributed H_2^+ molecular ions by a Bessel beam is independent of the TAM projection m of the twisted light. However, the cross section $d\sigma^{\rm tw}/d\Omega_f$ obviously depends on the opening angle θ_k. This can be seen in Fig. 3, in which the angle-differential cross section (27) is displayed as a function of the photon energy. Results for an incident plane-wave radiation (12) along the z axis are compared with Bessel beams with opening angles $\theta_k = 5^\circ$ and 30°, respectively. Cross sections are shown for three selected pairs of angles (ϑ_f,φ_f) of the emitted photoelectrons (cf. the rows of Fig. 3). In these computations, moreover, the H_2^+ molecular ions were assumed to be initially aligned along three different angles $\gamma = 0^\circ$ (left column), $\gamma = 45^\circ$ (middle column), and $\gamma = 90^\circ$ (right column) with regard to the z axis.

In the left column of Fig. 3, in particular, the H_2^+ molecular ions are aligned along the direction of the incident light ($\gamma = 0^\circ$). For this alignment, the plane-wave and twisted cross sections both oscillate and exhibit in general a rather similar behavior as a function of the photon energy. These oscillations in the angle-differential cross sections, if taken as a function of the photon energy, arise from the interference of the quantum amplitudes due to the photoionization of the electron

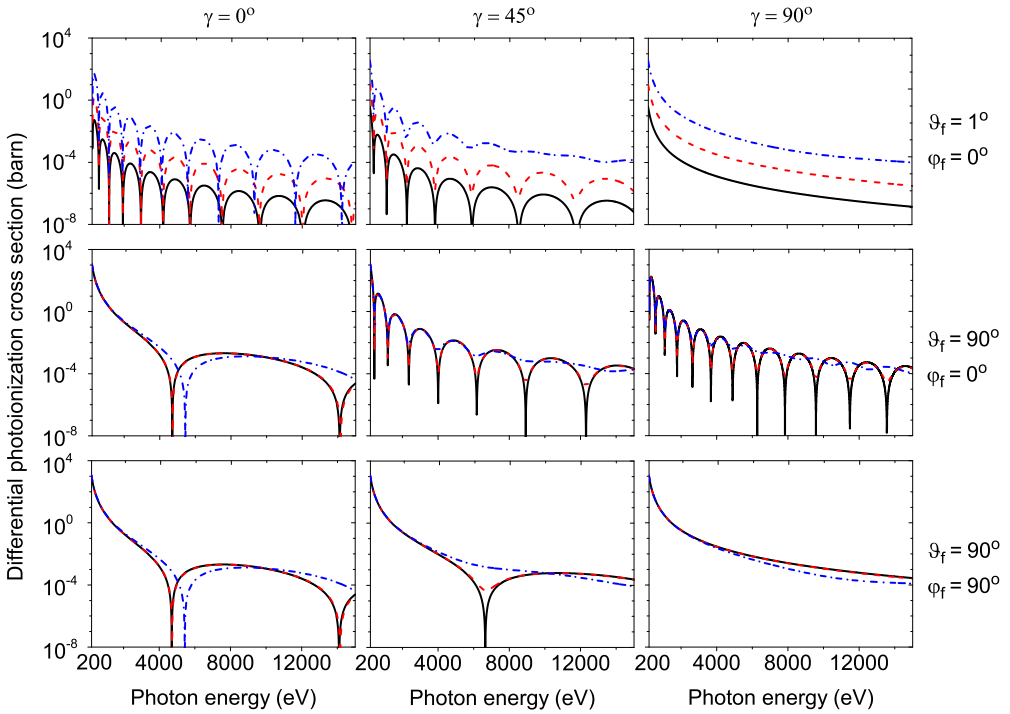

FIG. 3. (Color online) Angle-differential photoionization cross sections as a function of the photon energy of the incident light. Results are presented for selected angles (ϑ_f, φ_f) of the emitted electrons as well as for different orientations of the molecules. Cross sections (12) for incident plane waves (black solid lines) are compared with those for Bessel beams (27) with opening angles $\theta_k = 5^\circ$ (red dashed lines) and $\theta_k = 30^\circ$ (blue dash-dotted lines), respectively.

from the two nuclear centers of the molecules. A destructive interference (in the paths of the outgoing electron) leads to the pronounced minima in the cross sections as discussed previously [7]. For twisted Bessel light, the positions of these minima are shifted in general and now also depend on the opening angle θ_k of the beams.

More pronounced differences between the angle-differential cross sections $d\sigma^{\rm pl}/d\Omega_f$ and $d\sigma^{\rm tw}/d\Omega_f$ are found if the molecular axis is tilted by some angle $\gamma \neq 0^\circ$ with regard to the z axis. In the middle ($\gamma = 45^\circ$) and right ($\gamma = 90^\circ$) columns of Fig. 3, for example, the differential cross sections for the ionization by twisted light oscillate (much) less than for the plane-wave ionization, especially at high photon energies as well as for the large opening angles θ_k. An almost monotonic decrease of $d\sigma^{\rm tw}/d\Omega_f$ as a function of energy is found for $\theta_k = 30^\circ$ and $\vartheta_f = \varphi_f = 90^\circ$. For plane waves, in contrast, a clear minimum in the cross section at $\hbar\omega = 6.5$ keV is still found for the same alignment of the molecules ($\gamma = 45^\circ$).

This qualitative change in the angle-differential cross sections can be explained by the intensity profile of the Bessel beam due to its longitudinal component of the Poynting vector $P_z(r_\perp) = c_{+1}^2 J_{m-1}^2(\varkappa r_\perp) - c_{-1}^2 J_{m+1}^2(\varkappa r_\perp)$, where the coefficients $c_{\pm 1}$ were defined in Eq. (33) of Ref. [15]. Such an intensity profile is obviously not constant but exhibits a ringlike pattern as shown in Fig. 4. In this figure, the orange and blue rings refer to high and low intensity in line with the maxima and zeros of the Bessel functions $J_{m\pm1}(\varkappa r_\perp)$ of the first kind. For sufficiently small photon energy, the size of these rings is (much) larger than the internuclear distance R (cf. the left panel of Fig. 4) and hence the atomic centers of the H_2^+ ions are effectively exposed to the same intensity of the incident radiation, like for plane waves also. The angle-differential cross sections therefore show for both plane-wave and twisted Bessel beams a quite similar energy behavior for all photon energies $\hbar\omega < 3$ keV. At higher photon energies, in contrast,

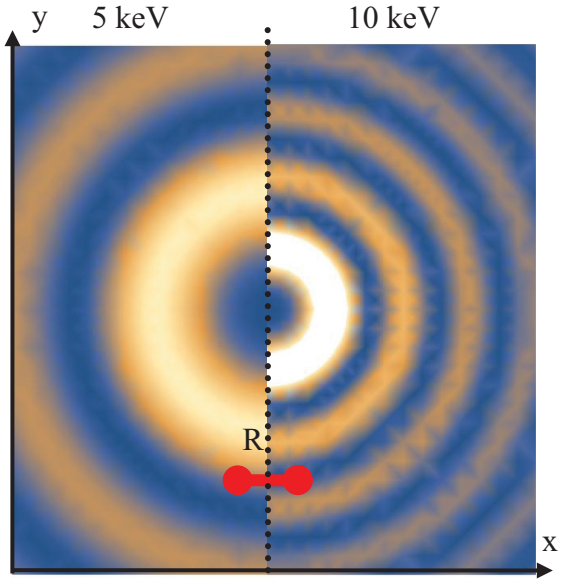

FIG. 4. (Color online) Transverse intensity profile of a Bessel beam with opening angle $\theta_k = 30^\circ$, projection of the TAM $m = 3$, helicity $\lambda = 1$, and for the two photon energies $\hbar\omega = 5$ keV (left) and $\hbar\omega = 10$ keV (right). For comparison, we also display the size of a H_2^+ molecular ion; see the text for further discussion.

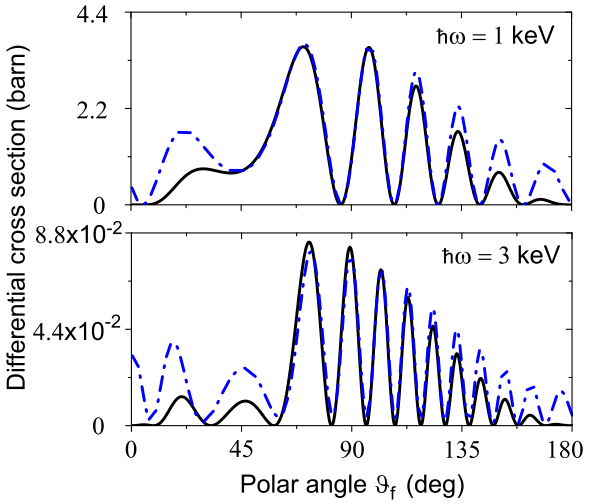

FIG. 5. (Color online) Angle-differential photoionization cross section as a function of the polar angle ϑ_f (of the detector) for H_2^+ molecular ions, aligned under the angle $\gamma = 45^\circ$, and if the photoelectrons are observed in the xz plane ($\varphi_f = 0^\circ$). Plane-wave results (black solid lines) are compared with the photoionization by means of a Bessel beam with opening angle $\theta_k = 30^\circ$ (blue dash-dotted lines) and are shown for the photon energies $\hbar\omega = 1$ keV (top) and $\hbar\omega = 3$ keV (bottom).

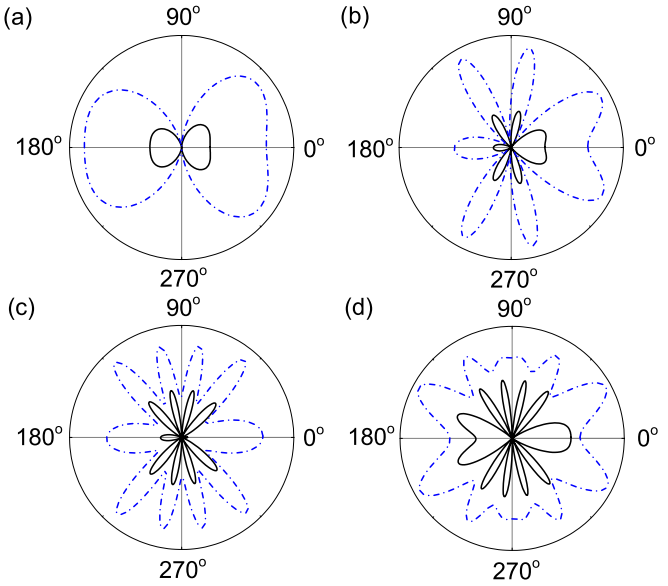

FIG. 6. (Color online) Comparison of the photoelectron angular distribution as a function of the angle φ_f for incident plane waves (black solid lines) and Bessel beams with opening angle $\theta_k = 30^\circ$ (blue dash-dotted lines). The H_2^+ molecular ions are assumed to be aligned again under the angle $\gamma = 45^\circ$ with regard to the z axis. Results in arbitrary units are shown for four different photon energies: (a) $\hbar\omega = 0.5$ keV, (b) $\hbar\omega = 3$ keV, (c) $\hbar\omega = 7$ keV, and (d) $\hbar\omega = 10$ keV. The polar angle of emitted electrons $\vartheta_f = 20^\circ$ is fixed.

the ringlike intensity varies over a smaller spatial extent and in particular for rather large opening angles θ_k, and the different nuclei are thus exposed to a different strength (intensity) of the radiation field. For this reason then, the interference pattern gradually disappear, similar to Young's experiment for double slits of nonequal widths.

So far, we have discussed the (angle-)differential cross section for the photoionization of H_2^+ ions as a function of the photon energy but for fixed angles (ϑ_f, φ_f) of the emitted electrons. To analyze also the angular dependence of $d\sigma^{\rm tw}/d\Omega_f$, Fig. 5 displays the cross sections as a function of polar angle ϑ_f of the photoelectrons for two different photon energies. In these computations, both the alignment ($\gamma = 45^\circ$) and azimuthal angle of the emitted electrons ($\varphi_f = 0^\circ$) are fixed. As can be seen from Fig. 5, the differential cross section $d\sigma^{\rm tw}/d\Omega_f$ does not longer vanish for $\vartheta_f = 0^\circ$, in contrast to an incident plane wave. This effect can be explained by the polarization (vector) of the twisted light, since the differential cross sections $d\sigma^{\rm pl,tw}/d\Omega_f \sim |\boldsymbol{e}_{\boldsymbol{k}\lambda} \cdot \boldsymbol{p}_f|^2$ are always proportional to the scalar product of the polarization vector and the propagation direction of the emitted electrons. For plane waves with $\boldsymbol{k} \parallel \boldsymbol{e}_z$, the polarization vector (13) is always perpendicular to the z axis and thus $|\boldsymbol{e}_{\boldsymbol{k}\lambda} \cdot \boldsymbol{p}_f|^2 \sim \sin^2\vartheta_f$ or $d\sigma^{\rm pl}/d\Omega_f|_{\vartheta_f=0^\circ} \simeq 0$. For twisted light (19), in contrast, the polarization vector also has a nonzero z component in the forward direction $\vartheta_f = 0^\circ$ and $d\sigma^{\rm tw}/d\Omega_f \neq 0$ in this case. For similar reasons, moreover, the cross section for twisted light is generally larger than for plane waves if $\vartheta_f = 1^\circ$, as can be seen from the top row of Fig. 3.

Finally, we can consider the angle-differential cross sections $d\sigma^{\rm tw}/d\Omega_f$ also as a function of the azimuthal angle φ_f of the emitted photoelectrons. In Fig. 6 we compare the corresponding angular distributions as functions of φ_f for plane waves (black solid lines) with those of Bessel beams with opening angle $\theta_k = 30^\circ$ (blue dash-dotted lines). Here the H_2^+ molecular ions are assumed to be aligned again under the angle $\gamma = 45^\circ$ with regard to the z axis. As can be seen from this figure, the two cross sections $d\sigma^{\rm tw}/d\Omega_f$ and $d\sigma^{\rm pl}/d\Omega_f$ exhibit a quite similar φ_f dependence at small photon energies. For $\hbar\omega = 0.5$ keV, for example, the shapes of the angular distribution are almost identical at the given polar angle $\vartheta_f = 20^\circ$, apart from their absolute values [cf. Fig. 6(a)]. In particular, the electron emission vanishes for $\varphi_f = 90^\circ$ for incident plane-wave radiation as well as for the Bessel beam. However, these (two) relative distributions start to deviate from each other if either the photon energy or the opening angle θ_k (not shown here in this figure) increases. For a photon energy of $\hbar\omega = 10$ keV, the Bessel beam results in a quite isotropic φ_f distribution of the emitted photoelectrons and in contrast to the well-defined lobes for plane-wave radiation of the same energy [cf. Fig. 6(d)]. Again, these modifications in the φ_f angular distribution can be understood from the intensity pattern of the corresponding Bessel beams, relative to the size of the H_2^+ molecular ions.

IV. SUMMARY AND OUTLOOK

A theoretical study has been performed for the photoionization of H_2^+ molecular ions by twisted Bessel light. The nonrelativistic first-order perturbation theory was applied to derive and analyze the angle-differential photoionization cross sections for photon energies for which the emitted electrons can be described in the first-order Born approximation. In this analysis, a macroscopic target of randomly distributed

but aligned H_2^+ molecular ions was assumed throughout the derivations. For such a target, it was shown that the angle-differential cross section $d\sigma^{\rm tw}/d\Omega_f$ is sensitive to the ratio of the transverse to the longitudinal momenta of the incident Bessel beam $\tan\theta_k = \varkappa/k_z$, while it remains independent of the projection m of the TAM. Detailed calculations of the angle-differential cross sections have been carried out for a different alignment γ of the H_2^+ ions and for different photon energies of the incident Bessel light to see how these properties affect the oscillations in the cross sections as known for incident plane-wave radiation. The main modifications in the angular distribution of the photoelectrons hereby arise due to the (ringlike) pattern of Bessel beams and their intensity variation relative to the size of the H_2^+ molecular ions. Hence, the photoionization of diatomic molecules by twisted radiation opens up different possibilities for the investigation of atomic double-slit phenomena. The use of twisted photons will allow one to perform a molecular analog of Young's experiment with two slits of unequal widths.

While the angle-differential photoionization cross sections occur to be insensitive with regard to (the projection of the) TAM m for any macroscopic target, even if the molecular ions are supposed to be aligned, such an m dependence is expected if the size of the target becomes comparable to the variations in the transverse intensity pattern of the Bessel beams. The analysis of the Young-type interference behavior of the energy and angular distribution of emitted photoelectrons can therefore provide accurate information about the twisted nature of the photon beams. The investigation of photoionization of H_2^+ molecular ions from the localized targets, displaced relative to the beam axis of the incident radiation, is left for future work.

[1] I. G. Kaplan and A. P. Markin, Zh. Eksp. Teor. Fiz. **64**, 424 (1973) [JETP **37**, 216 (1973)].
[2] M. Walter and J. Briggs, J. Phys. B **32**, 2487 (1999).
[3] H. D. Cohen and U. Fano, Phys. Rev. **150**, 30 (1966).
[4] B. Zimmermann *et al.*, Nat. Phys. **4**, 649 (2008).
[5] M. V. Frolov, N. L. Manakov, S. S. Marmo, and A. F. Starace, J. Mod. Opt. **62**, S28 (2015).
[6] I. Sanchez and F. Martin, Phys. Rev. A **57**, 1006 (1998).
[7] A. S. Baltenkov, U. Becker, S. T. Manson, and A. Z. Msezane, J. Phys. B **45**, 035202 (2012).
[8] D. Akoury *et al.*, Science **318**, 949 (2007).
[9] M. Ilchen *et al.*, Phys. Rev. Lett. **112**, 023001 (2014).
[10] G. Molina-Terriza, J. P. Torres, and L. Torner, Nat. Phys. **3**, 305 (2007).
[11] J. Bahrdt, K. Holldack, P. Kuske, R. Müller, M. Scheer, and P. Schmid, Phys. Rev. Lett. **111**, 034801 (2013).
[12] S. Sasaki and I. McNulty, Phys. Rev. Lett. **100**, 124801 (2008).
[13] E. Hemsing, A. Marinelli, and J. B. Rosenzweig, Phys. Rev. Lett. **106**, 164803 (2011).
[14] H. He, M. E. J. Friese, N. R. Heckenberg, and H. Rubinsztein-Dunlop, Phys. Rev. Lett. **75**, 826 (1995).
[15] O. Matula, A. G. Hayrapetyan, V. G. Serbo, A. Surzhykov, and S. Fritzsche, J. Phys. B **46**, 205002 (2013).
[16] J. Durnin, J. J. Miceli, Jr., and J. H. Eberly, Phys. Rev. Lett. **58**, 1499 (1987).
[17] J. Arlt and K. Dholakia, Opt. Commun. **177**, 297 (2000).
[18] H. M. Scholz-Marggraf, S. Fritzsche, V. G. Serbo, A. Afanasev, and A. Surzhykov, Phys. Rev. A **90**, 013425 (2014).
[19] A. Surzhykov, D. Seipt, V. G. Serbo, and S. Fritzsche, Phys. Rev. A **91**, 013403 (2015).
[20] S. Stock, A. Surzhykov, S. Fritzsche, and D. Seipt, Phys. Rev. A **92**, 013401 (2015).
[21] M. Babiker, C. R. Bennett, D. L. Andrews, and L. D. Romero, Phys. Rev. Lett. **89**, 143601 (2002).
[22] G. F. Quinteiro and P. I. Tamborenea, Europhys. Lett. **85**, 47001 (2009).
[23] U. D. Jentschura and V. G. Serbo, Phys. Rev. Lett. **106**, 013001 (2011).
[24] A. Afanasev, C. E. Carlson, and A. Mukherjee, Phys. Rev. A **88**, 033841 (2013).
[25] B. H. Bransden and C. J. Joachain, *Physics of Atoms and Molecules* (Prentice Hall, Harlow, 2003).
[26] O. A. Fojón, J. Fernández, A. Palacios, R. D. Rivarola, and F. Martín, J. Phys. B **37**, 3035 (2004).
[27] J. Fernández, O. Fojón, and F. Martín, Phys. Rev. A **79**, 023420 (2009).
[28] L. Argenti *et al.*, New J. Phys. **14**, 033012 (2012).
[29] H. A. Bethe and E. E. Salpeter, *Quantum Mechanics of One- and Two-Electron Atoms* (Springer, Berlin, 1957).
[30] G. N. Watson, *Theory of Bessel Functions* (Cambridge University Press, Cambridge, 1966).